System Identification Technique for Active Helicopter Rotors

SANG JOON SHIN,[1,*] CARLOS E. S. CESNIK[2] AND STEVEN R. HALL[3]

[1]*School of Mechanical and Aerospace Engineering, Seoul National University, Seoul 151-742, Korea*
[2]*Department of Aerospace Engineering, University of Michigan, Ann Arbor, MI 48109, USA*
[3]*Department of Aeronautics and Astronautics, Massachusetts Institute of Technology, Cambridge, MA 02139, USA*

ABSTRACT: System identification methodology is developed for a linear time-periodic (LTP) system and applied to an experimental setup of an integrally twist-actuated helicopter rotor blade. Identification is conducted for a controller design, which alleviates vibratory loads induced in forward flight. Since a rotor in forward flight is a time-periodic system due to the aerodynamic environment varying once per rotation, the adopted methodology requires determination of the multicomponent harmonic transfer functions. A simplified identification formula is also derived for a linear time-invariant (LTI) system, such as a rotor system in hover. The latter approach gives another estimate of the primary component among the harmonic transfer functions. The identification experiment is conducted at NASA Langley Transonic Dynamics Tunnel. The magnitude of the higher-order harmonic transfer functions is observed to be small in the frequency range of interest when compared with that of the primary component. This indicates that the present active rotor system may be regarded as a LTI system under the level flight conditions considered. Results obtained in system identification are interpreted in terms of the closed-loop controller design.

Key Words: system identification, linear time-periodic system, blade integral actuation, helicopter vibration, vibration control, wind tunnel test.

INTRODUCTION

ACTIVE control upon the helicopter rotors has been investigated extensively over the last few decades, and those studies were to accomplish low vibration and acoustic noise-emitting helicopter rotors. Several control schemes, which actuate either the swashplate or individual blade pitch at higher harmonic frequencies, have been developed and tested (Ham, 1987; Shaw et al., 1989). They were based on the idea of directly modifying unsteady aerodynamic loads acting upon the rotor blades. However, typical disadvantages were also observed from those traditional active control approaches. Recently, active materials have enabled much more efficient implementation of active controls on helicopters, using multiple lightweight sensors/actuators embedded or surface-mounted at several locations in rotor blades (Friedmann, 1997; Loewy, 1997; Chopra, 2000). Various mechanisms have been suggested for active materials application to the helicopter vibration reduction (Giurgiutiu, 2000). From the feasibility tests, potential capabilities about helicopter vibration reduction were substantiated for a number of mechanisms proposed (Rodgers and Hagood, 1998; Cesnik et al., 1999; Prechtl and Hall, 2000; Bernhard and Chopra, 2002). These achievements encourage to design and implement an appropriate closed-loop controller for helicopter vibratory load reduction.

For successful design of a closed-loop controller, it is essential to obtain the transfer function relationship between the fixed-system loads and blade actuation in advance. Traditionally, a T-matrix approach has been used to identify such transfer functions by the researchers who studied conventional active control (Molusis et al., 1983; Shaw et al., 1989). In this approach, only discrete component at target frequency, i.e., $N\Omega$, among the transfer function was identified from sine-dwell open-loop actuation and used in the controller design. However, to improve the controller design through preliminary evaluation of closed-loop system stability, further system identification results are also required in the vicinity of the target frequency. Recently, transfer function relationship for some prototypes of active rotor blade was identified experimentally over a certain frequency range by sine-sweep actuation (Rodgers and Hagood, 1998; Prechtl and Hall, 2000; Bernhard and Chopra, 2002). All those tests and the corresponding identification were conducted in hover condition. Helicopter rotor is a linear time-invariant (LTI) system in hover. Therefore, there was no need to take into

*Author to whom correspondence should be addressed.
E-mail: ssjoon@snu.ac.kr

1045-389X/05/11/12 1025–14 $10.00/0 DOI: 10.1177/1045389X05053916

account any further complicacy that originated from forward flight condition. An identification approach based on a LTI system was developed and used in those experiments. While helicopter rotor is a time-invariant system in hover, it becomes time-periodic during forward flight due to periodicity in aerodynamics. Furthermore, it is known that the characteristics of linear time-periodic (LTP) system can be completely described by multicomponent harmonic transfer functions (Wereley and Hall, 1991; Nitzsche, 2001). A practical system identification methodology has been recently established and suggested to estimate such multicomponent harmonic transfer functions for helicopter rotor in forward flight (Siddiqi and Hall, 2001).

Among the active material mechanisms suggested for helicopter vibration reduction, the integral twist actuation concept is selected for blade control in this study. A comprehensive investigation on the helicopter integral blade actuation has been conducted under the NASA/Army/MIT Active Twist Rotor (ATR) program. It is a collaborative research effort between the US Army Research Laboratory, at NASA Langley Research Center, and the University of Michigan/MIT. During the program, analysis and design capabilities were developed, active blades were manufactured, and open-loop forward flight tests were conducted. Details of the activities are described in the following: structural modeling of the integral blades (Cesnik et al., 1999; Cesnik and Shin, 2001a); blade design, prototyping, and its bench test (Cesnik et al., 1999); hover test and its correlation with analysis (Wilbur et al., 2000; Cesnik et al., 2001b); open-loop forward flight test and its correlation with analysis (Wilbur et al., 2002a,b); acoustic noise investigation in the open-loop forward flight test (Booth and Wilbur, 2002); and a preliminary numerical simulation of the closed-loop control (Shin et al., 2002). During the open-loop forward flight test, significant impact upon both fixed- and rotating-system loads was observed from a prescribed blade twist actuation (Wilbur et al., 2002a). These achievements motivate a system identification effort for a closed-loop controller design on the ATR system.

This article presents a system identification approach that allows the characterization of the behavior of an active helicopter rotor for which control laws must be developed. The NASA/Army/MIT ATR system in forward flight is the subject of the experimental part of this study. First, a LTP system and its identification methodology adopted in this study are introduced. Then, a simplified identification formula for a LTI system is presented. The sine-sweep signal generated for identification, and the numerical implementation of the identification algorithms are described in detail. Finally, the identification results are presented from both approaches for a LTP system and a LTI system. The results are interpreted in view of a future control law design.

FUNDAMENTALS OF A LTP SYSTEM

In a LTP system, a sinusoid input at single frequency ω generates a superposition of sinusoids at several frequencies of various amplitudes and phases. The multiple output frequencies are the input frequency modulated by the plant frequency ω_P, i.e., $\omega, \omega+\omega_P, \omega-\omega_P, \omega+2\omega_P, \omega-2\omega_P, \ldots$ Although the number of frequencies to be superposed is theoretically infinite, they may be truncated for practical purposes, and the smallest number of them are retained, which adequately represents the system dynamics. Consider, for example, that only three frequencies in the output are to be accounted for. Then, the output Y comprises of the linear combination of the responses due to inputs at frequencies ω, $\omega+\omega_P$, and $\omega-\omega_P$. This is equivalent to considering the system output as a linear combination of three different harmonic transfer functions (each corresponding to one of the three frequencies): G_0, G_{+1}, and G_{-1}, respectively. Thus,

$$Y(j\omega) = G_0(j\omega)\cdot U(j\omega) + G_{+1}(j\omega)\cdot U(j\omega - j\omega_P) + G_{-1}(j\omega)\cdot U(j\omega + j\omega_P) \quad (1)$$

A linear system represented by Equation (1) is depicted in the block diagram in Figure 1. However, since there is only one equation available in order to estimate three transfer functions G_0, G_{+1}, and G_{-1}, the identification problem becomes underdetermined. This leads to the need for three different input applications, in order to obtain three independent equations, each of which is similar to Equation (1). Due to the periodic nature of the plant under consideration, it is important to account for the time of application of each input relative to the plant period T. In order for the plant behavior to be completely analyzed, multiple identical input signals are

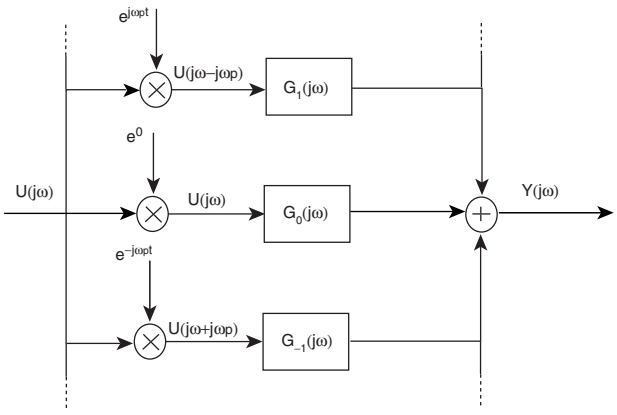

Figure 1. *LTP system block diagram with three harmonic transfer functions.*

applied, which are evenly distributed over the plant period. An example of the input signals is shown in Figure 2. Here, three input signals are created in sine-sweep (chirp) form with uniformly separated initiation interval T_d over the plant period T, where

$$T_d = T/3 = 2\pi/3\omega_P \tag{2}$$

Among the three input signals, the first one should have no delay between the start of the plant period and its initiation time. Then, the input U and output Y_0 can be modeled as in Figure 1. For the second signal, there should be a delay T_d seconds between them, and the input can be described as $U(j\omega)e^{-j\omega T_d}$, which results in a block diagram, shown in Figure 3. Similarly, the delay for the third signal is $2T_d$. Then, the vector of outputs Y can be expressed as:

$$\begin{Bmatrix} Y_0 \\ Y_{1/3} \\ Y_{2/3} \end{Bmatrix} = \begin{bmatrix} U(j\omega) & U(j\omega - j\omega_P) & U(j\omega + j\omega_P) \\ U(j\omega) & U(j\omega - j\omega_P)W & U(j\omega + j\omega_P)W^{-1} \\ U(j\omega) & U(j\omega - j\omega_P)W^2 & U(j\omega + j\omega_P)W^{-2} \end{bmatrix} \times \begin{Bmatrix} G_0 \\ G_{+1} \\ G_{-1} \end{Bmatrix} \tag{3}$$

where $Y_{1/3}$ and $Y_{2/3}$ are the outputs due to the second and third chirp signals, respectively. Also, W is used with the definition that $W = e^{j\omega_P T_d} = e^{j2\pi/3}$. Equation (3) can be simply written as:

$$Y = U \cdot G \tag{4}$$

or to compute the harmonic transfer functions directly

$$G = U^{-1} \cdot Y \tag{5}$$

The derivation so far is based on the assumption that the output measurements due to each input signal must be conducted by allowing the response to settle down significantly before the next input signal is initiated. Then, it can be assumed that Y_0 is only due to the first input, $Y_{1/3}$ due to the second input, and so on. However, to make the identification process faster, input signals with less non-actuation time between successive signals are preferred. This leads to the idea of treating the entire input sequence as a single input signal, and similarly for the output signal. However, this will once more render the problem underdetermined. Further assumptions on the characteristics of G are required to make the problem well-defined. Therefore, a methodology to estimate harmonic transfer functions is adopted, which makes the problem constrained with these additional assumptions.

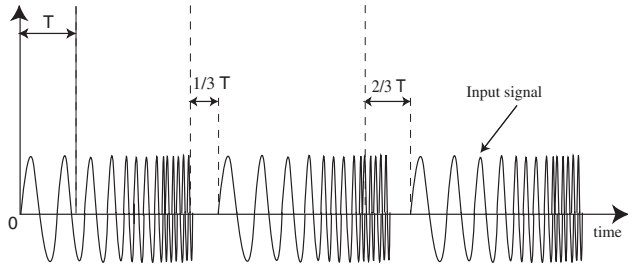

Figure 2. *Input signal generated with appropriate time intervals over the plant period.*

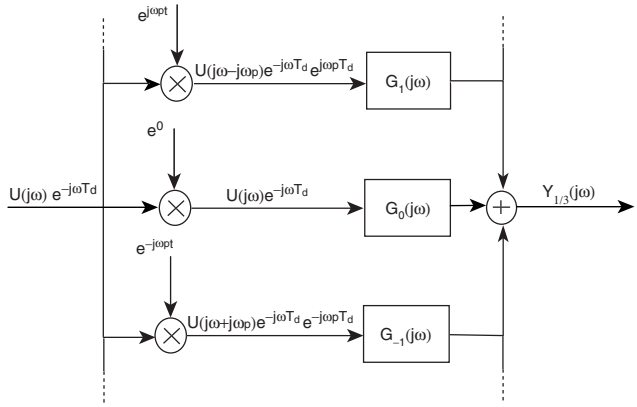

Figure 3. *Delayed input signal and corresponding output of LTP system.*

IDENTIFICATION OF A LTP SYSTEM

The general characteristics of the LTP system described in the previous section, require three sets of data, namely the input u, output y, and time measurements ψ (at which u and y occur) for its identification. For rotor system identification, the information of ψ can be extracted from the record of the azimuth measurements. These data are recorded during the experiment in a discrete manner with some fixed sampling frequency. Therefore, all the data can be assembled in a vector of length n, where n is the total number of the data points. The input data can be expressed as:

$$\begin{bmatrix} u_1 & u_2 & u_3 & \cdots & u_n \end{bmatrix} \tag{6}$$

y and ψ are similarly defined. If the harmonic transfer functions of the system as many as n_h need to be identified, an $n_h \times n$ matrix $\mathbf{U}$ is constructed according to Equation (3), with an appropriately modulated and Fourier transformed vector $\mathbf{u}$ at each row as follows:

$$\mathbf{U} = \begin{bmatrix} \mathbf{u}(\omega - m\omega_P) & \cdots & \mathbf{u} & \cdots & \mathbf{u}(\omega + m\omega_P) \end{bmatrix}^T \tag{7}$$

where $m = (n_h - 1)/2$. Similarly, $\mathbf{Y}$ can be constructed as the discrete Fourier transform of the vector y as

$$\mathbf{Y} = \mathcal{F}\{\begin{bmatrix} y_1 & y_2 & y_3 & \cdots & y_n \end{bmatrix}\} \tag{8}$$

Recalling that the empirical transfer function estimate of a LTI system involves the power and cross spectral densities of the input and output, these spectral densities

can be defined in a similar manner for the LTP system as:

$$\begin{aligned}\mathbf{\Phi}_{\mathbf{UU}} &= \mathbf{U}^*\mathbf{U} \\ \mathbf{\Phi}_{\mathbf{UY}} &= \mathbf{U}^*\mathbf{Y}\end{aligned} \tag{9}$$

where $\mathbf{U}^*$ is complex conjugate transpose of $\mathbf{U}$. Then, the transfer functions can be obtained for LTP system similarly as in LTI system as:

$$\mathbf{G}(\omega) = (\mathbf{\Phi}_{\mathbf{UU}})^{-1}\mathbf{\Phi}_{\mathbf{UY}} \tag{10}$$

where $\mathbf{G}(\omega)$ is the transfer function estimate with each harmonic transfer function G_i at its row as:

$$\mathbf{G}(\omega) = \begin{bmatrix} G_{+m} & \cdots & G_{+1} & G_0 & G_{-1} & \cdots & G_{-m} \end{bmatrix}^{\mathrm{T}} \tag{11}$$

Notice, however, that the computation of the transfer function based on Equation (10) will not yield an accurate result since only a few harmonics are considered instead of an infinite number. The cumulative effect of the neglected harmonics may be significant. Assume that a given system has inherently N_{h} transfer functions of significant magnitudes, but only n_{h} of them are evaluated. Then, its output can be expressed as:

$$\begin{aligned}\mathbf{Y} &= \sum_{k=-m}^{m} \mathbf{u}(\omega - k\omega_{\mathrm{P}})G_k + \mathbf{e} \\ &= \mathbf{U}^{\mathrm{T}}\mathbf{G} + \mathbf{e}\end{aligned} \tag{12}$$

where the unmodeled part essentially appears as the error $\mathbf{e}$. In addition to this modeling error, the identification problem is still underdetermined. To solve this problem, an assumption is made that the transfer functions are relatively smooth, so it does not present drastic variations with frequency. This generates a minimization problem with a cost function J, which penalizes a quadratic error and the curvature of the transfer functions, so that

$$J = \min\left[\left(\mathbf{Y} - \mathbf{U}^{\mathrm{T}}\mathbf{G}\right)^2 + \alpha\left(\mathbf{D}^2\mathbf{G}\right)^2\right] \tag{13}$$

where $\mathbf{D}^2$ is a second-order differential operator, and α is a weighting factor. That is, the penalty term penalizes the curvature of the transfer function. Taking the derivative of J with respect to $\mathbf{G}$ in Equation (13) and setting it to zero, the minimizing $\mathbf{G}$ can be found as:

$$\mathbf{G} = \left[\mathbf{U}^{\mathrm{T}}\mathbf{U} + \alpha\mathbf{D}^4\right]^{-1}\mathbf{U}^{\mathrm{T}}\mathbf{Y} \tag{14}$$

where $\mathbf{D}^4 = \mathbf{D}^2 \cdot \mathbf{D}^2$. Equation (14) is one of the formulas utilized in the system identification conducted in this study. Other issues on the practical implementation of Equation (14) and its solutions are provided in Siddiqi and Hall (2001).

SIMPLIFIED FORMULA FOR A LTI SYSTEM

General characteristics of a LTP system and its identification methodology are described in detail in the previous sections. For a LTI system, such as a helicopter rotor system in hover, a much more simplified formula can be applied for the identification of its transfer function. In this section, a practical identification methodology for a LTI system is briefly presented, based on the one that was developed for an active rotor system with trailing edge flaps in hover (Prechtl and Hall, 2000). For a LTP system, the methodology presented in this section provides a result with regard to only the primary component among the harmonic transfer functions, i.e., G_0. Hence it will enable a comparison between the results obtained from both methodologies, regarding G_0.

An empirical transfer function estimate for a LTI system is obtained by taking a division of the Fourier transform of the output and input signals. This division tends to be dominated by noise, and hence the estimate becomes inaccurate. Thus the collection of sine-sweep response is averaged in the frequency domain using cross- and auto-spectra, to eliminate part of the noise. If the Fourier transform of the output and input signals are given by $Y(f)$ and $U(f)$, respectively, the averaged cross-spectrum is expressed as:

$$\widehat{\phi_{yu}} = \frac{1}{N}\sum_{i=1}^{N} Y_i(f)U_i^*(f) \tag{15}$$

where i is the index of a particular sine-sweep signal set and N is the total number of the sine-sweeps. Similarly, the auto-spectrum of the input is obtained as:

$$\widehat{\phi_{uu}} = \frac{1}{N}\sum_{i=1}^{N} U_i(f)U_i^*(f) \tag{16}$$

An average transfer function is given by

$$\overline{G_0}(f) = \frac{\widehat{\phi_{yu}}}{\widehat{\phi_{uu}}} \tag{17}$$

Smoothing scheme is then applied to the averaged cross- and auto-spectra by taking convolution of those signals in the frequency domain with a smoothing window. A Bartlett window is a well-known function to give the best results in terms of smoothing the transfer function while maintaining the details of the transfer function. The smoothed cross- and auto-spectra are expressed as:

$$\begin{aligned}\widehat{\widehat{\phi_{yu}}} &= \widehat{\phi_{yu}} * h_{\mathrm{b}}(f) \\ \widehat{\widehat{\phi_{uu}}} &= \widehat{\phi_{uu}} * h_{\mathrm{b}}(f)\end{aligned} \tag{18}$$

where $h_b(f)$ is the Bartlett window. The expression of the Bartlett window used is

$$h_b(f) = \frac{1}{\gamma_s}\left(\frac{\sin(\gamma_s/2k_s)f}{\sin(1/2k_s)f}\right)^2 \tag{19}$$

where the constant k is used to normalize the frequency values in the argument of the sine functions. The actual Bartlett window used to smooth the experimental identification results in this study is shown in Figure 4. The smoothed transfer function is obtained by taking the division of the smoothed cross- and auto-spectra as follows:

$$\overline{\overline{G_0}}(f) = \frac{\widehat{\widehat{\phi_{yu}}}}{\widehat{\widehat{\phi_{uu}}}} \tag{20}$$

Averaging the sine-sweep response results will always lead to an accurate estimate of the transfer function and can be performed without limit. However, smoothing must be applied carefully since too much smoothing can lead to an overestimate on the system damping. The parameters defining the shape of the Bartlett window used are chosen to give a smooth transfer function estimate while capturing the dominant details of the transfer function result, as indicated by the averaged transfer function result. Engineering judgment will be used in applying the smoothing scheme.

A complementary estimate of the transfer function is obtained by computing

$$\overline{G_0'}(f) = \frac{\widehat{\phi_{yy}}}{\widehat{\phi_{uy}}} \tag{21}$$

The division of $\overline{G_0}(f)$ by $\overline{G_0'}(f)$ gives the coherence of a transfer function estimate. Numerical values of coherence vary between zero and unity. The coherence of a transfer function will be low if there is an excessive noise in the system or if the system behaves nonlinearly. Except for some friction and material nonlinearities in the embedded integral actuators, the active rotor experimental system may be regarded as linear. Thus, the region with low coherence indicates that there is a large amount of aerodynamic noise existing at corresponding frequencies. By use of the identification methodologies presented in this section, additional information can be obtained regarding the coherence of a transfer function estimate.

GENERATION OF A SINE-SWEEP SIGNAL

As described in the previous section, sinusoids are used to determine transfer functions, and more specifically, sine-sweep waves (chirp signals) are used to obtain the system response over a specific range of frequencies. The chirps may have frequencies that vary linearly, quadratically, or logarithmically with time. The frequency content and time interval of the chirp is dependent on the system characteristics. It is also important to take into account the chirp phase in the case of an LTP system.

For a helicopter rotor system with b blades and rotor period $T_r = 2\pi/\Omega$, the system period T becomes T_r/b. Then, the output frequencies due to an input signal at ω

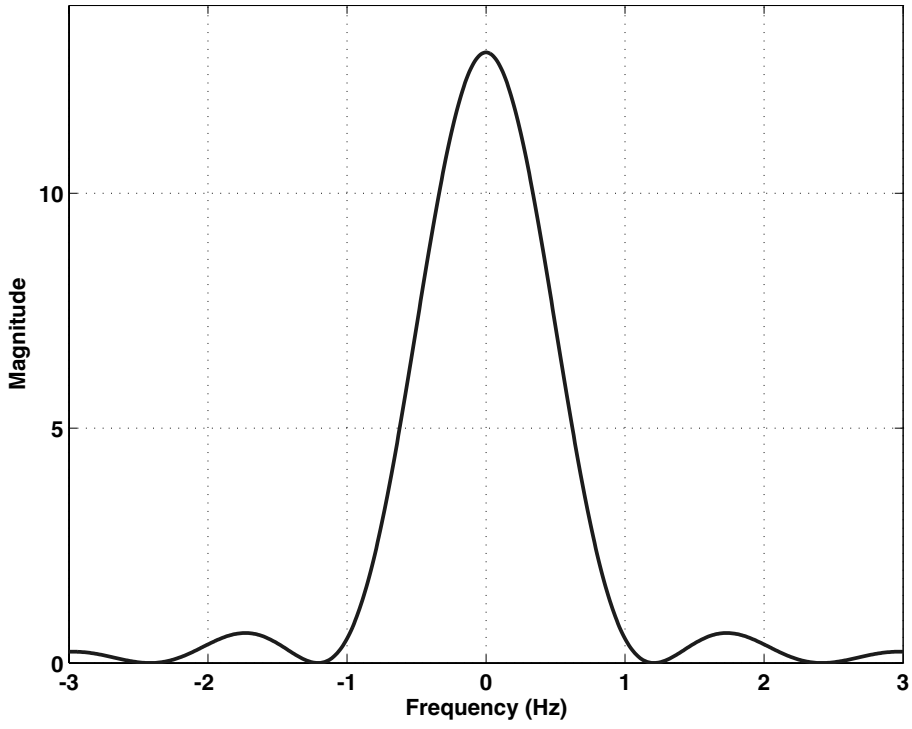

Figure 4. *Typical Bartlett window used to smooth the experimental results.*

will be shifted by positive and negative multiples of the blade passage frequency ω_P, where

$$\omega_P = 2\pi b/T_r \tag{22}$$

Since a linearly varying sine-sweep signal is considered in the present system identification test, the frequencies of the input signal are a linear function of time, so that

$$f = f_0 + \frac{f_1 - f_0}{T_c} t \tag{23}$$

where f_0 is the initial frequency (Hz), f_1 is the final frequency (Hz), and T_c is period of the sine-sweep (summation of t_d, single actuation period, and t_p, non-actuation period between two successive actuations). Frequencies of 5 and 70 Hz are selected for the numerical values of f_0 and f_1, respectively, in order to include frequencies up to 6P. Integration of the frequency equation, Equation (23), gives the phase angle of the chirp, ϕ_c as:

$$\phi_c(t) = \left(f_0 t + \frac{f_1 - f_0}{2T_c} t^2 \right) 2\pi \tag{24}$$

where the phase is in radians. The sine-sweep signal is generated using the unwrapped azimuth location measurements. The relation between the rotor rotational speed Ω (rpm) and the azimuth location ψ is

$$\psi = \frac{360}{60} \Omega t \tag{25}$$

where time t is in seconds. A pseudo-time $\hat{t}$ is introduced here. Uniformly distributed phase of N chirps over 360° can be constructed by considering the number of chirps that have already been generated, n_c, and shifting the time vector accordingly.

$$\hat{t} = \left[\psi - \left\{ -360 + \mathrm{mod}\left(360 \frac{n_c}{N}, 360 \right) \right\} \right] \frac{60}{360\,\Omega} \tag{26}$$

where 'mod' is the modulo function that returns the remainder from the division of two arguments. The constructed chirp signal vector $\mathbf{U}_c$ with amplitude A_c for the rotor system may be expressed as:

$$\mathbf{U}_c = A_c \sin\left[2\pi \phi_c(\hat{t}) \right] \mathbf{V} \tag{27}$$

where $\mathbf{V}$ is a vector of length N. Collective, cyclic, and differential modes of blade actuation can be generated by adjusting the components of $\mathbf{V}$. In the case of the present four-bladed ATR system, $\mathbf{V}$ becomes $[1\ 1\ 1\ 1]^T$ for collective mode, while $[1\ -1\ 1\ -1]^T$ for differential mode.

It is expected that the vibration-reducing controller will be designed to suppress only the hub normal shear component. Thus, only the normal component from the rotor fixed-system balance is extracted and used as a reference signal $\mathbf{z}(\mathbf{t})$ for the closed-loop control. (See the definition of $\mathbf{z}(\mathbf{t})$ in Equation (28).) Unfortunately, at the beginning, an unidentified electrical problem causes this channel to be noisy. In particular, there are 'spikes' or transients in the signal, which induces the control system to produce control signals that are unrealistically large, and which does not reduce vibration. To eliminate this problem, a non-linear filter is developed to identify and remove these transients in real-time.

EXPERIMENTAL SETUP FOR SYSTEM IDENTIFICATION

The experiments for the system identification of the ATR system are conducted at the Transonic Dynamics Tunnel (TDT) at NASA Langley Research Center. The Aeroelastic Rotor Experimental System (ARES) helicopter testbed is also used in the test. The unique characteristics of the TDT and the ARES testbed are described in detail in Wilbur et al. (2002a). Figure 5 shows the ATR test blades mounted on the ARES helicopter testbed in the TDT.

All the system identification tests are conducted in the heavy gas medium of the TDT at a nominal density of 2.432 kg/m^3. The rotor rotational speed throughout the test is held at 688 rpm, resulting in a nominal hover tip Mach number of 0.60. The rotor speed does vary

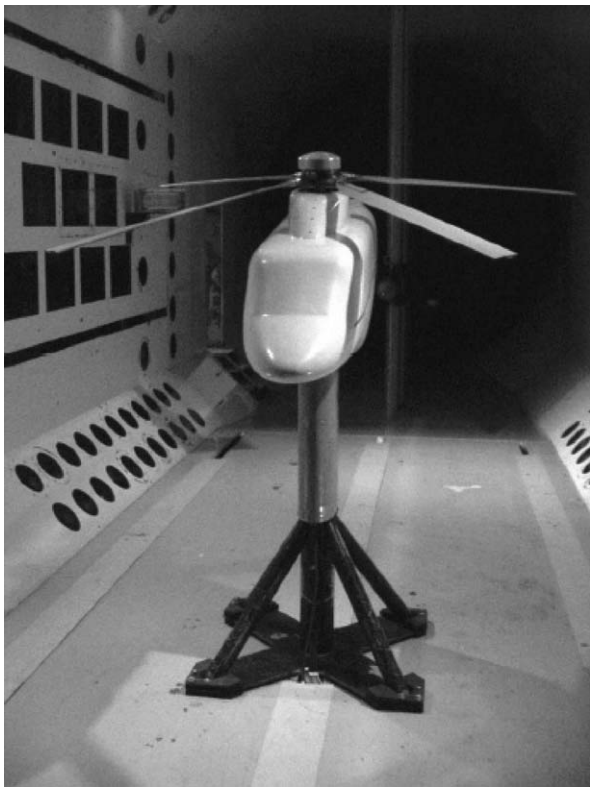

Figure 5. *The ARES testbed inside the TDT with ATR test blade installed.*

slightly during the open-loop test. The small drifts in rotor speed are accounted for in the identification algorithms.

The flight conditions used in the tests are representative of helicopters in forward flight (Table 1). For each flight condition, the rotor is trimmed to a nominal thrust coefficient C_T of 0.0066. The rotor is considered to be trimmed when the first harmonic of blade flapping is $<0.1^\circ$ (Wilbur et al., 2002a). This condition is referred to as 'baseline.' The data corresponding to the baseline condition are acquired first, and then the constructed chirp signal is applied to the ATR system. The data from the ARES testbed fixed-system balance, blade built-in strain gauges and accelerometer, and the high-voltage amplifier channels are recorded at a rate of 4000 samples per second. The signals acquired during the test are listed in Table 2. Among them, the ARES 1P signal extracted from the rotor control system is composed of sharp peaks indicating the instant that Blade No. 1 passes through 0° azimuth location. This provides the azimuth information for the system identification.

Using the sine-sweep signals established in the previous section, various modes (collective, longitudinal cyclic, lateral cyclic, and differential) of chirp actuation signal are ready to build and apply with the amplitude of 1000 V and nine phase angle divisions over 360°. Due to a high sampling frequency, and many channels of simultaneous acquisition being used, data corresponding to each phase angle division must be saved separately before proceeding to the next phase. Figure 6 shows the block diagram of Simulink code used in the test that generates the sine-sweep signals for system identification.

Table 1. Forward flight conditions for the system identification test.

	$\mu = 0.140$	$\mu = 0.200$	$\mu = 0.267$	$\mu = 0.333$
$\alpha_S = -1^\circ$	X	X		
$\alpha_S = -2^\circ$			X	
$\alpha_S = -6^\circ$				X

Table 2. Data acquisition during the system identification test.

Signal	Components
Rotor fixed-system balance	Axial, normal, pitch, roll, side, yaw
Active blade instrumentation	Six torsion, one chordwise bending, three flap bending, tip acceleration
Rotor system control	ARES 1P
Voltage	Blade-1
Current	Blade-1

NUMERICAL IMPLEMENTATION OF IDENTIFICATION ALGORITHM

Before applying the system identification algorithm developed in the previous section, the amplitude of the baseline loads must be subtracted from those under actuation. This is due to the definition of the transfer matrix that will be used in the foregoing closed-loop controller design, as represented by the following equation:

$$\mathbf{z} = \mathbf{z}_o + \mathbf{T}\mathbf{u} \tag{28}$$

where $\mathbf{z}$ is a vector of vibration amplitudes, $\mathbf{T}$ is the transfer matrix, $\mathbf{u}$ is the vector of the actuation amplitudes, and $\mathbf{z}_o$ is the vector of the vibration amplitudes with no actuation (baseline). For this reason, the ATR system loads in baseline condition are acquired before applying blade actuation in each flight condition tested. Such baseline loads are then manipulated to give the average values in terms of the azimuth locations. Results of the averaged baseline fixed-system balance loads in the condition $\mu = 0.333$ are exemplified in Figures 7 and 8.

Since the load data under sine-sweep actuation are saved separately for each phase division, those must be concatenated into a single array before the system identification algorithm is applied. To maintain a correct periodicity in the array generated, load data prior to the first and beyond the last ARES 1P peaks are discarded during the concatenation. In the test, 20-s duration is selected for t_d, single actuation period, and 4-s for t_p, non-actuation period between two successive actuations, respectively. As a result, nine successive chirps (each with a difference phase) generate an array

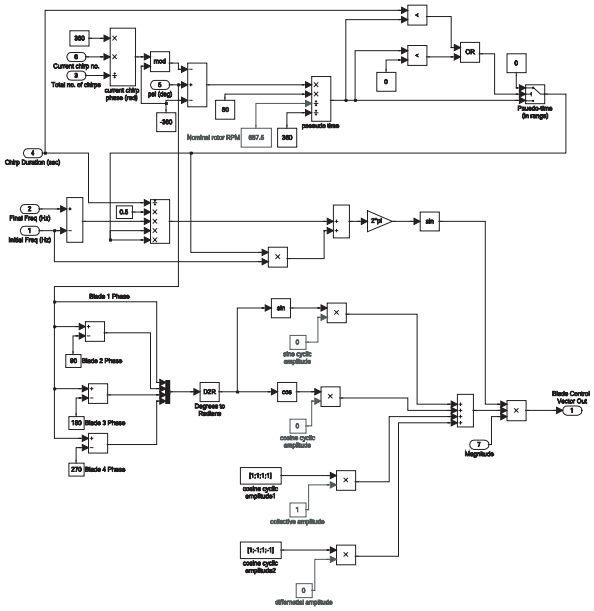

Figure 6. *Simulink model of the sine-sweep input signal generator.*

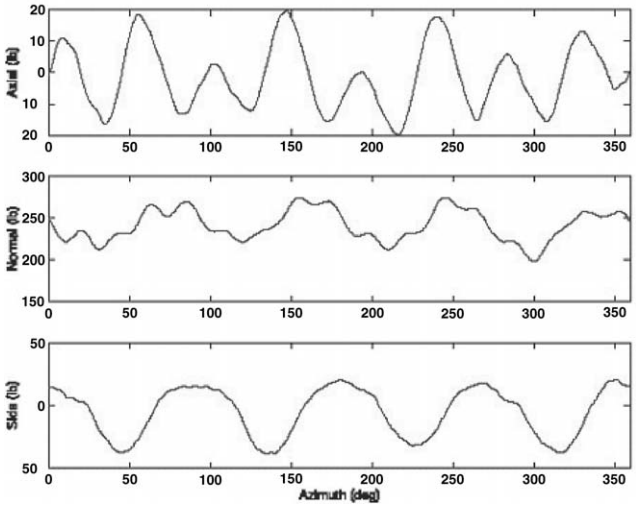

Figure 7. *Shear force component of the averaged baseline fixed-system loads in the condition $\mu = 0.333$.*

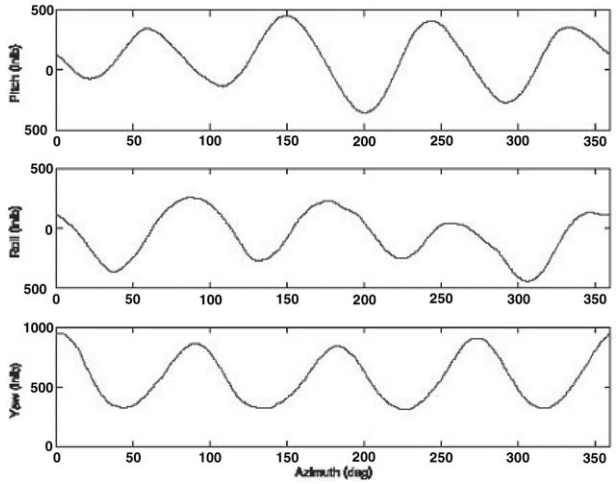

Figure 8. *Moment component of the averaged baseline fixed-system loads in the condition $\mu = 0.333$.*

$\approx$200 s long, which is $<$216 s, i.e., $(20+4)\times 9$. Furthermore, three sets of the chirp test are repeated for the same condition during the test, and used to estimate an averaged result on the harmonic transfer functions.

Furthermore, drifts in the rotor rotational speed is taken into account during the identification process. Varying torques on the rotor system causes the rotor rotational speed to vary from its prescribed value (688 rpm). Such an instantaneous rotor speed variation makes the length of data record to be saved either shorter or longer than the correct length. Data with different lengths may give an incorrect frequency domain result after the Fourier transformation is applied. Therefore, the data record length is checked against the correct length per each revolution, and adjusted to give the correct length using interpolation technique. One of the arrays concatenated from the three sets of hub normal shear data is shown in Figure 9 for the collective blade actuation case and for the flight condition $\mu = 0.333$, $\alpha_S = -6^\circ$, $C_T = 0.0066$. Since the baseline loads are subtracted, the hub normal shear now oscillates around 0 lb, not 225 lb, the thrust corresponding to $C_T = 0.0066$. At the same time, the high-voltage chirp input signal applied to the blade-embedded actuators is concatenated and manipulated in a similar fashion for the system identification algorithm.

As mentioned here, three different sets of data are acquired for each test condition. Harmonic transfer function results obtained from each set are averaged to construct the final results. In addition, after three data sets are acquired for the broad frequency range (5–70 Hz), the same condition is tested with a narrow frequency range of actuation. The narrow frequency range is used to obtain more accurate harmonic transfer function results near 4P. Thus, 40 and 52 Hz are selected for the initial and final frequencies in the test, since 4P corresponds to 46 Hz in the case of the ATR system. Harmonic transfer function results from these narrow frequency range tests are also added to the average process mentioned here.

RESULTS FROM THE LTP SYSTEM METHODOLOGY

The system identification scheme developed for a generic LTP system is first applied to the concatenated input and output arrays with the weighting factor $\alpha = 10^{14}$ in Equation (14). Five harmonic transfer functions, G_{-2}, G_{-1}, G_0, G_{+1}, and G_{+2}, are estimated simultaneously. Results for the hub normal shear are shown in Figure 10 in the case of collective blade actuation and flight condition $\mu = 0.333$, $\alpha_S = -6^\circ$, $C_T = 0.0066$. The magnitudes of the five harmonic functions are shown in the figure; the phase is only shown for G_0. As can be seen in the figure, G_0 has an amplitude which is significantly larger than the others. Higher-order components of the harmonic transfer functions appear to be negligible. This indicates that the response of the ATR system may be described only by the G_0 component, behaving like a LTI system, for the particular flight condition and blade actuation considered here. More information about the blade dynamics can be also extracted from the G_0 result for the hub normal shear. It is observed that the peaks approximately match the frequencies of the rigid and elastic flap bending modes of the blade.

The harmonic transfer functions for cyclic actuation are shown in Figures 11 and 12. The results are similar to the results for collective actuation in that the G_0 response dominates. Therefore, the ATR system may be considered as being LTI for cyclic actuation as well.

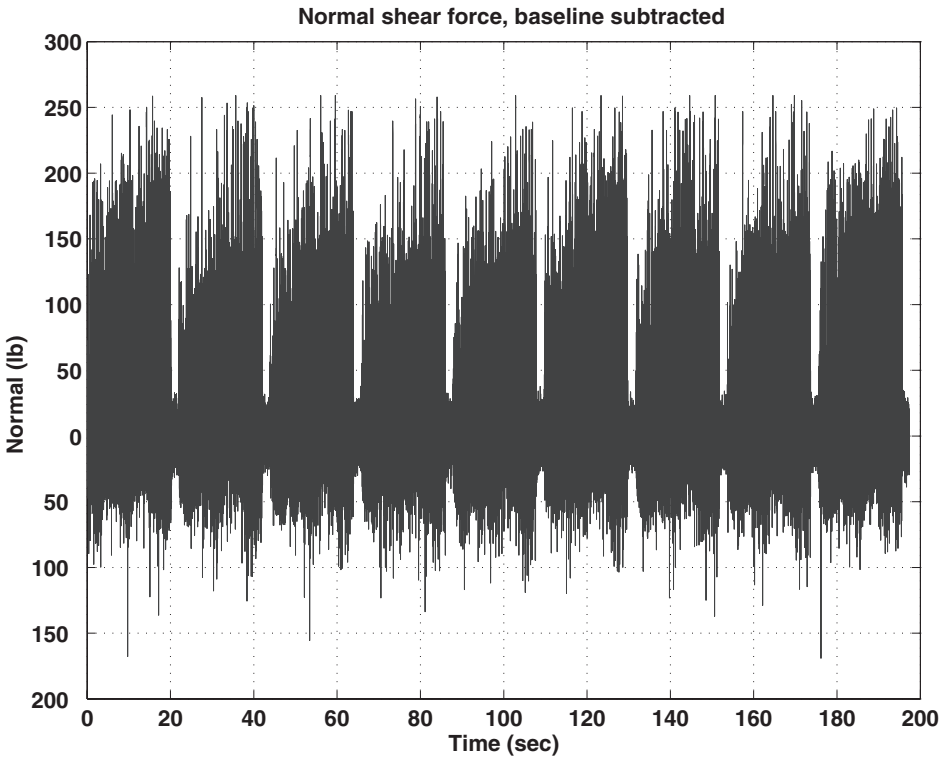

Figure 9. *Concatenated array of the hub normal shear force for collective actuation in the condition $\mu = 0.333$.*

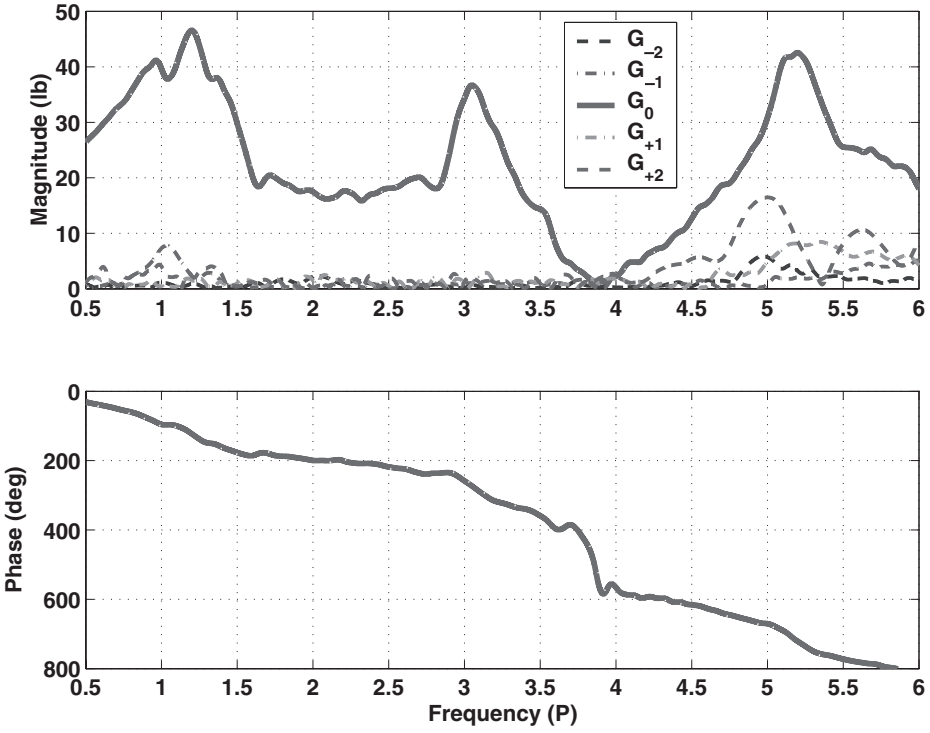

Figure 10. *Harmonic transfer functions of the hub normal shear force during the collective actuation for $\mu = 0.333$, $\alpha_S = -6^\circ$, $C_T = 0.0066$, and 1000 V twist actuation.*

Notice also that the two cyclic modes of actuation exhibit much more control authority at 4P, which is ≈10 lb for each mode, than the collective mode does, which is <2 lb. Thus, the two cyclic modes of blade actuation may be used more effectively in reducing 4P hub normal vibratory loads by the closed-loop controller for the level flight condition considered here. Ineffectiveness of the collective mode for 4P hub normal vibratory load reduction was already observed in the ATR open-loop forward flight experiment (Wilbur et al.,

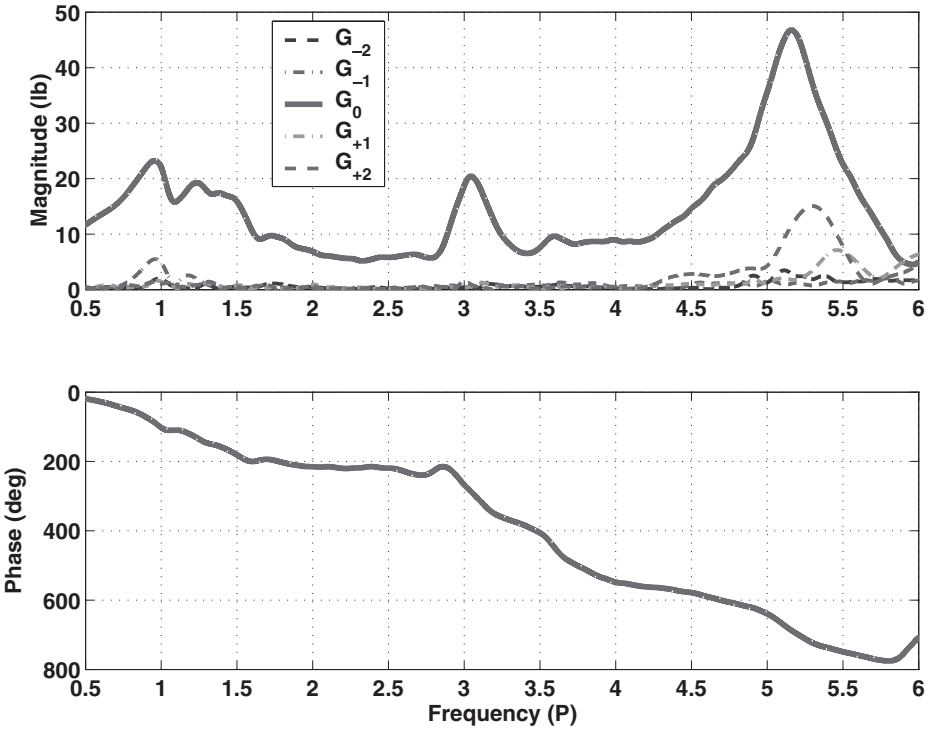

Figure 11. *Harmonic transfer functions of the hub normal shear force during the longitudinal cyclic actuation for $\mu = 0.333$, $\alpha_S = -6^\circ$, $C_T = 0.0066$, and 1000 V twist actuation.*

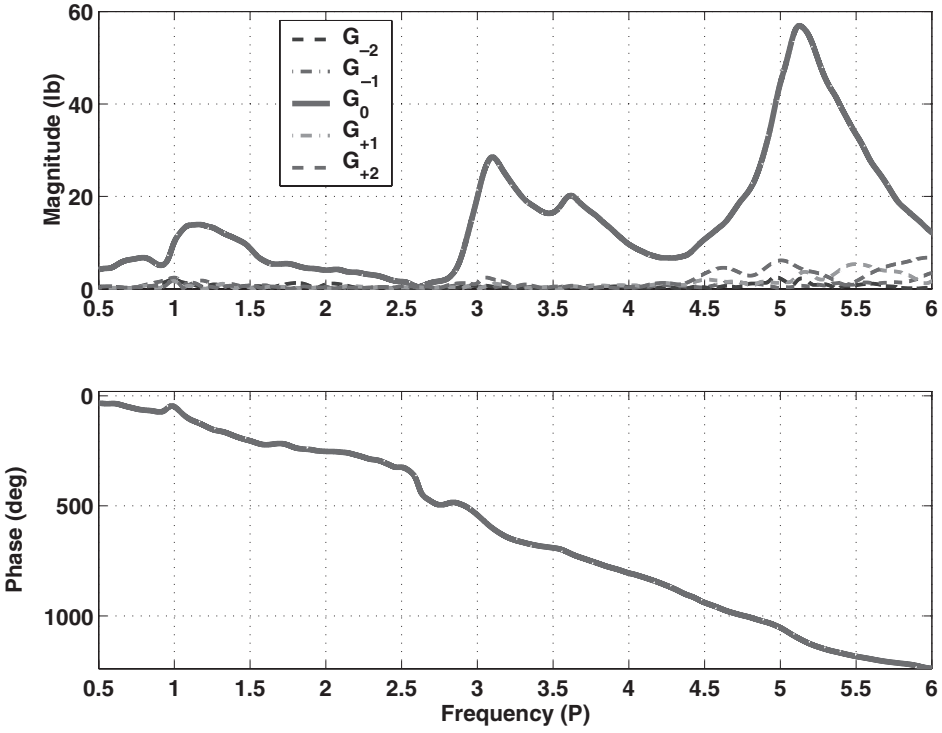

Figure 12. *Harmonic transfer functions of the hub normal shear force during the lateral cyclic actuation for $\mu = 0.333$, $\alpha_S = -6^\circ$, $C_T = 0.0066$, and 1000 V twist actuation.*

2002a,b). In the open-loop test, prescribed 4P IBC-mode actuation showed much less impact on the fixed-system loads than the other actuations used. Note that the 4P IBC-mode signal is exactly the same as the collective mode of actuation at 4P. However, significant control authority is found at 1P frequency in the ATR system from the collective mode of actuation. This suggests the possible use of the collective mode for alleviating 1P vibratory loads in the closed-loop controller, and therefore, improving blade tracking. The differential mode of actuation is not capable of affecting the hub normal shear, so it is excluded from the closed-loop controller.

Transfer function results for the hub normal shear obtained for different flight conditions are shown in Figure 13. Again, the G_0 component shows much larger amplitude than the other higher-order harmonic transfer functions in each flight condition and blade actuation mode used. Thus, only the magnitude results of the fundamental transfer function, G_0, are provided for different advance ratios. It is observed that the transfer function varies slightly with advance ratio. This suggests the possibility of using a single control law for all 1-g flight conditions. Therefore, based on the same numerical values obtained at one condition, the resulting closed-loop controllers are expected to exhibit similar levels of vibratory load reduction for different flight conditions.

RESULTS FROM THE SIMPLIFIED LTI APPROACH

The simplified formula developed for LTI system identification is applied to calculate the primary component among the harmonic transfer functions, i.e., G_0. Based on Equation (20), G_0 estimate for the hub normal shear is obtained as shown in Figure 14 in the case of collective blade actuation and flight condition $\mu = 0.333$, $\alpha_S = -6^\circ$, $C_T = 0.0066$. The G_0 results for the magnitude and phase show good agreement with those obtained using the LTP system methodology in the previous section. Low coherence region appears near 4P frequency, which indicates that a large amount of aerodynamic noise is transferred through the hub to the

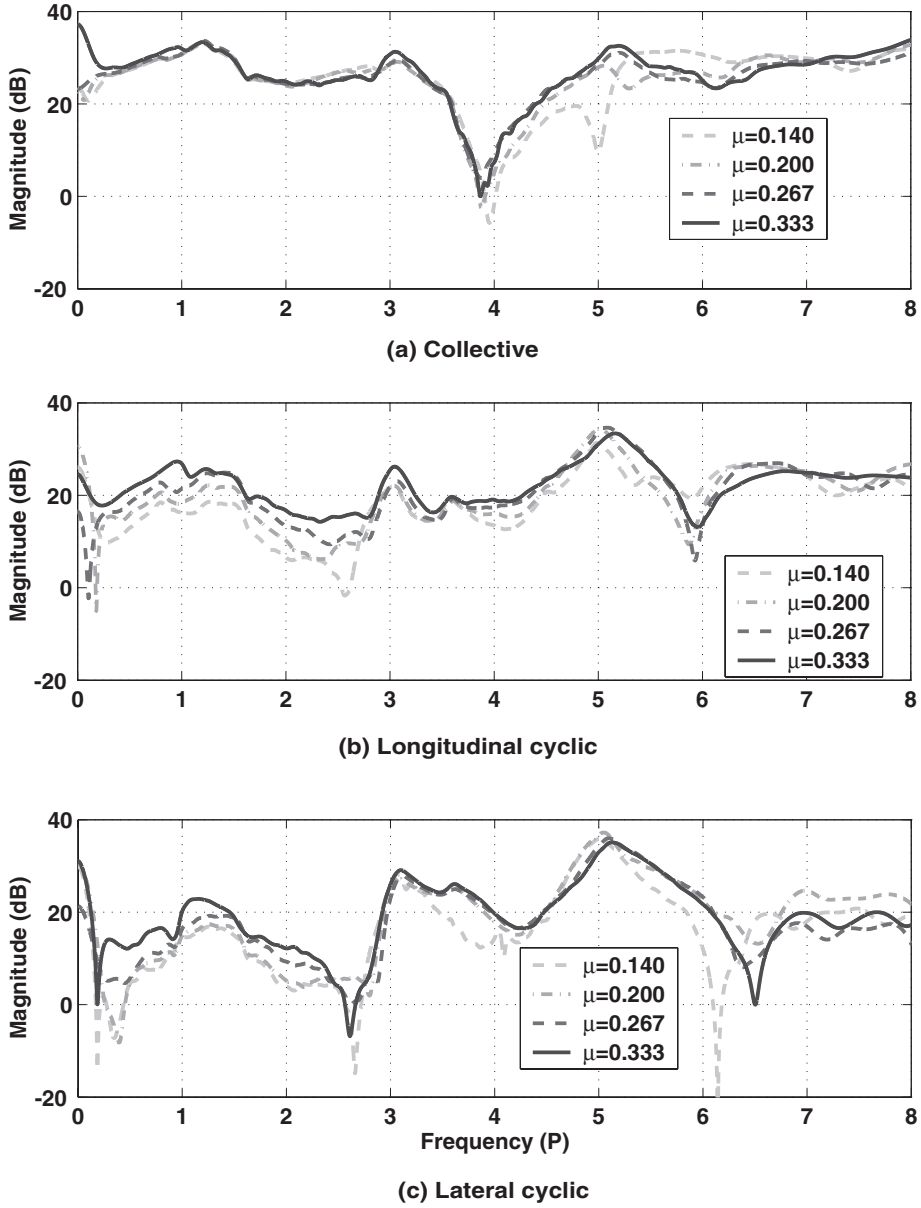

Figure 13. *Transfer functions (magnitude only) of the hub normal shear force during the three actuation modes for $\mu = 0.140$, 0.200, 0.267, 0.333, and 1000 V twist actuation.*

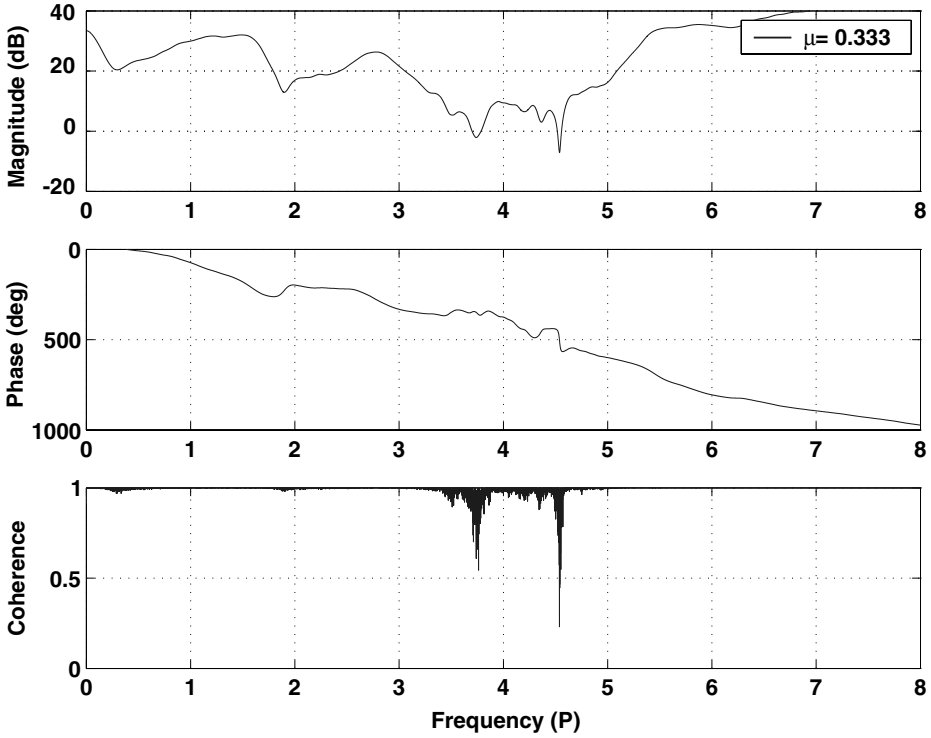

Figure 14. *Transfer function of the hub normal shear force during the collective actuation mode for $\mu = 0.333$, and 1000 V twist actuation.*

fixed system near at that frequency. This observation also justifies the present identification technique of using a narrow frequency range of actuation, around 4P frequency, to obtain an accurate transfer function result.

Harmonic transfer function results are obtained for the other components of the fixed-system loads. Similar dominance of G_0 is observed in these cases as well. Therefore, a simplified formula can be applied equivalently to estimate G_0. The G_0 magnitude results for the hub pitching moment are shown in Figure 15 for the flight condition $\mu = 0.333$, $\alpha_S = -6^\circ$, $C_T = 0.0066$, and 1000 V twist actuation. Control authority on the hub pitching moment is considerable at the 4P frequency for all three modes of actuation. This indicates that a potentially desirable use of this actuation authority is for vehicle performance improvement rather than vibratory load reduction. For example, a combination of 1P collective and cyclic actuation may develop additional pitching moment for the helicopter pull-up maneuver. Also, modified 1P collective and cyclic actuation can be used to relieve the power required for forward flight by preventing or delaying rotor stall in the retreating side of the rotor blades. A study on helicopter performance enhancement achieved by blade twist actuation is currently being conducted by the authors (Shin and Cesnik, 2003).

Control authority obtained at discrete frequency of interest, such as 4P, from the present system identification is used as a design parameter in the closed-loop controller. However, before implementing a controller in the experimental setup, it will be more desirable to perform a preliminary stability prediction on the closed-loop system in an analytical way. Since complete transfer function result is obtained in this study, reliable analytical estimation on the system stability is available. It is also possible to further improve the closed-loop controller design based on the preliminary stability prediction.

CONCLUSIONS

This article addresses the development of a system identification methodology for a LTP system and its application to an experimental system with integrally twisted helicopter rotors. Active helicopter rotor system is experimentally identified for its vibration control design. Forward flight conditions are selected since it generally induces helicopter vibration. Since aerodynamic environment acting on the blades exhibits periodicity during forward flight, an identification methodology developed for a generic LTP system must be adopted to identify characteristics of the rotor system. Harmonic transfer functions result from the LTP system methodology with their multiple components. A simplified approach for a LTI system is also used to give another estimate for the primary

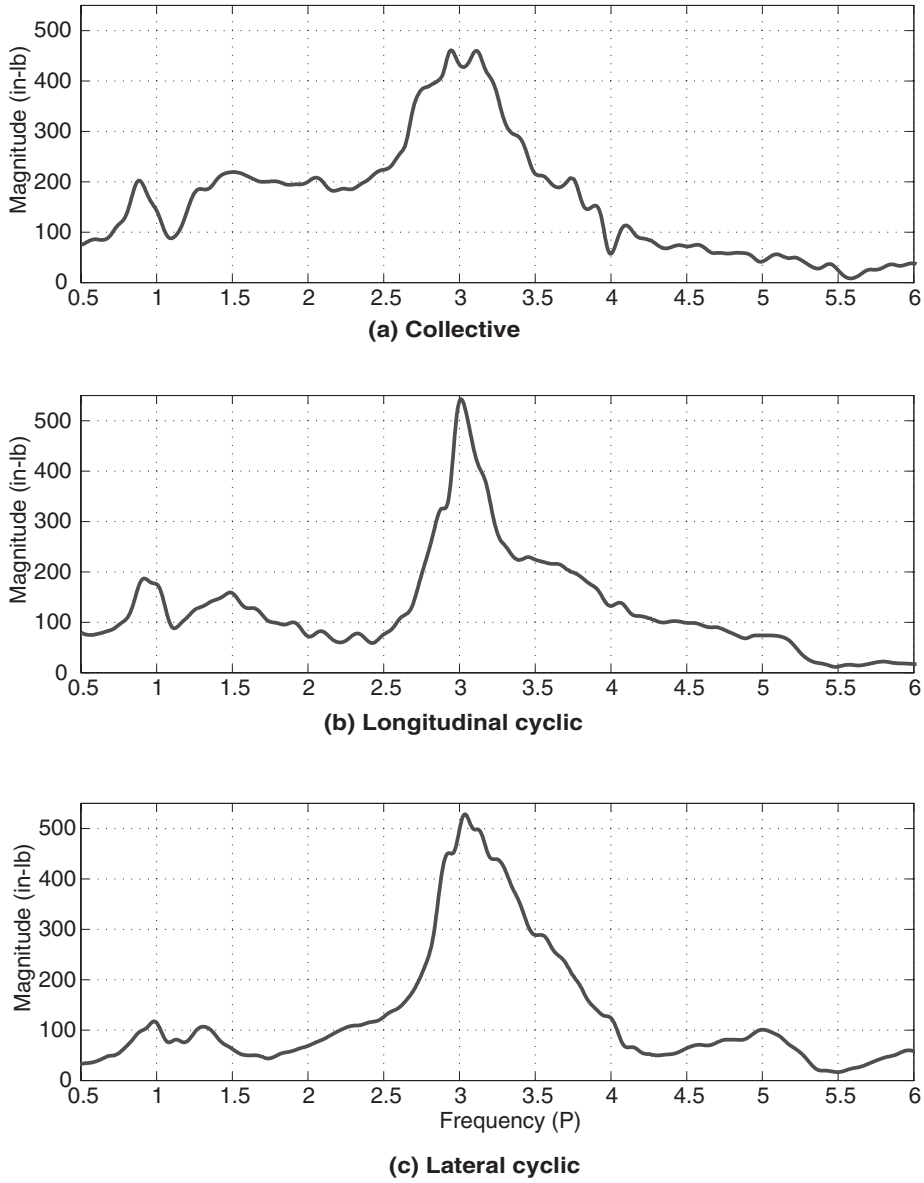

Figure 15. *Transfer functions (magnitude only) of the hub pitching moment during the three actuation modes for $\mu = 0.333$, $\alpha_S = -6^\circ$, $C_T = 0.0066$, and 1000 V twist actuation.*

component among the harmonic transfer functions, i.e., G_0. Blade sine-sweep actuation signal is generated for the experimental setup, which enables LTP system identification. As a result, G_0 shows much larger magnitude than the other higher-order components, such as G_{-2}, G_{-1}, G_{+1}, and G_{+2}. This signifies that the ATR system can be regarded as a LTI system under the level flight conditions and blade actuation modes considered in the test. Both identification approaches for a LTP system and a LTI system give a consistent estimate on G_0. The coherence result requires that a precise identification be performed near 4P frequency.

The two cyclic modes of actuation appear to be more effective than the collective mode does regarding the ATR 4P hub normal vibratory load. Combination of the two cyclic modes at 4P and the collective one at 1P is expected to give a considerable reduction in the ATR hub shear vibratory load. Therefore, multimode and multiharmonic structure is recommended for a closed-loop controller. The identified transfer function does not vary much as the flight condition changes. This suggests a possibility of designing and applying a common closed-loop controller to the various flight conditions. Control authority obtained for the other components of fixed-system loads, such as hub pitching moment may be utilized for vehicle performance enhancement. Before implementing a control law, it is desirable to check analytically the stability of the closed-loop system. System identification results enable such prediction since transfer function results are obtained over a range of frequencies in interest. It also enables improvement of the control law in case instability is predicted.

ACKNOWLEDGMENTS

The authors are especially thankful to Messrs. Matthew L. Wilbur, William T. Yeager, and Chester W. Langston (US Army Vehicle Technology Directorate, NASA Langley Research Center) for their support in conducting the wind tunnel tests, and to Dr. Kyungyeol Song (Department of Aeronautics and Astronautics, Massachusetts Institute of Technology) for providing help on the system identification methodology. This work was sponsored by NASA Langley Research Center under the cooperative agreement number NCC1-323, and also supported by the US Army Research Laboratory and the US Army Research Office under contract number DAAD19-01-1-0390.

REFERENCES

Bernhard, A.P.F. and Chopra, I. 2002. "Hover Test of a Mach-Scale Rotor Model with Active Blade Tips," *Journal of the American Helicopter Society*, 47(4):273–284.

Booth, E.R. and Wilbur, M.L. 2002. "Acoustic Aspects of Active Twist Rotor Control," In: *Proceedings of the American Helicopter Society 58th Annual Forum*, Montreal, Canada.

Cesnik, C.E.S., Shin, S.J., Wilkie, W.K., Wilbur, M.L. and Mirick, P.H. 1999. "Modeling, Design, and Testing of the NASA/Army/MIT Active Twist Rotor Prototype Blade," In: *Proceedings of the American Helicopter Society 55th Annual Forum*, Montreal, Canada.

Cesnik, C.E.S. and Shin, S.J. 2001a. "On the Modeling of Integrally Actuated Helicopter Blades," *International Journal of Solids and Structures*, 38(10–13):1765–1789.

Cesnik, C.E.S., Shin, S.J. and Wilbur, M.L. 2001b. "Dynamic Response of Active Twist Rotor Blades," *Smart Materials and Structrues – Special Issue on Rotorcraft Application*, 10:62–76.

Chopra, I. 2000. "Status of Application of Smart Structures Technologies to Rotorcraft Systems," *Journal of the American Helicopter Society*, 45(4): 228–252.

Friedmann, P.P. 1997. "The Promise of Adaptive Materials for Alleviating Aeroelastic Problems and Some Concerns," In: *Proceedings of the Innovation in Rotorcraft Technology*, London, United Kingdom.

Giurgiutiu, V. 2000. "Recent Advances in Smart Material Rotor Control Actuation," In: *Proceedings of AIAA/ASME/ASCE/AHS/ASC 41st Structures, Structural Dynamics and Materials Conference*, AIAA Paper No. 2000-1709, Atlanta, GA.

Ham, N.D. 1987. "Helicopter Individual-Blade-Control Research at MIT 1977–1985," *Vertica*, 11(1/2):109–122.

Loewy, R. 1997. "Recent Developments in Smart Structures with Aeronautical Applications," *Smart Materials and Structures*, 6: 11–42.

Molusis, J.A., Hammond, C.E. and Cline, J.H. 1983. "A Unified Approach to the Optimal Design of Adaptive and Gain Scheduled Controllers to Achieve Minimum Helicopter Rotor Vibration," *Journal of the American Helicopter Society*, 28(2):9–18.

Nitzsche, F. 2001. "Laplace-Domain Approximation to the Transfer Functions of a Rotor Blade in Forward Flight," *Aeronautical Journal*, 105(1077):233–240.

Prechtl, E.F. and Hall, S.R. 2000. "Design and Implementation of a Piezoelectric Servo-Flap Actuation System for Helicopter Rotor Individual Blade Control," AMSL Report #00-03, Active Materials and Structures Laboratory, Massachusetts Institute of Technology, Cambridge, MA.

Rodgers, J.P. and Hagood, N.W. 1998. "Development of an Integral Twist-Actuated Rotor Blade for Individual Blade Control," AMSL Report #98–6, Active Materials and Structures Laboratory, Massachusetts Institute of Technology, Cambridge, MA.

Shaw, J., Albion, N., Hanker, E.J. and Teal, R.S. 1989. "Higher Harmonic Control: Wind Tunnel Demonstration of Fully Effective Vibratory Hub Force Suppression," *Journal of the American Helicopter Society*, 31(1):14–25.

Shin, S.J., Cesnik, C.E.S. and Hall, S.R. 2002. "Control of Integral Twist-Actuated Helicopter Blades for Vibration Reduction," In: *Proceedings of the American Helicopter Society 58th Annual Forum*, Montreal, Canada.

Shin, S.J. and Cesnik, C.E.S. 2003. "Helicopter Performance and Vibration Enhancement by Twist-Actuated Blades," In: *Proceedings of AIAA/ASME/ASCE/AHS/ASC 44th Structures, Structural Dynamics and Materials Conference*, AIAA Paper No. 2003-1357, Norfolk, VA.

Siddiqi, A. and Hall, S.R. 2001. "Identification of the Harmonic Transfer Functions of a Helicopter Rotor," AMSL Report #01-01, Active Materials and Structures Laboratory, Massachusetts Institute of Technology, Cambridge, MA.

Wereley, N.M. and Hall, S.R. 1991. "Linear Time Periodic Systems: Transfer Functions, Poles, Transmission Zeros and Directional Properties," In: *Proceedings of 1991 American Control Conference*, Boston, MA.

Wilbur, M.L., Yeager, W.T., Jr., Wilkie, W.K., Cesnik, C.E.S. and Shin, S.J. 2000. "Hover Testing of the NASA/Army/MIT Active Twist Rotor Prototype Blade," In: *Proceedings of the American Helicopter Society 56th Annual Forum*, Virginia Beach, VA.

Wilbur, M.L., Mirick, P.H., Yeager, W.T., Jr., Langston, C.W., Cesnik, C.E.S. and Shin, S.J. 2002a. "Vibratory Loads Reduction Testing of the NASA/Army/MIT Active Twist Rotor," *Journal of the American Helicopter Society*, 47(2):123–133.

Wilbur, M.L., Yeager, W.T., Jr., and Sekula, M.K. 2002b. "Further Examination of the Vibratory Loads Reduction Results from the NASA/Army/MIT Active Twist Rotor Test," In: *Proceedings of the American Helicopter Society 58th Annual Forum*, Montreal, Canada.